ARTICLE NO. 79-4137

Flight Through Thunderstorm Outflows

Walter Frost*
FWG Associates, Inc., Tullahoma, Tenn.
Bill Crosby†
Arnold Engineering and Development Center, Tullahoma, Tenn.
and
Dennis W. Camp‡
NASA George C. Marshall Space Flight Center, Huntsville, Ala.

Computer simulation of aircraft landing through thunderstorm gust fronts is carried out. The 3 degree-of-freedom, nonlinear equations or aircraft motion for the longitudinal variables containing all two-dimensional wind shear terms are solved numerically. The gust front spatial wind field inputs are provided in the form of tabulated experimental data which are coupled with a computer table lookup routine to provide the required wind components and shear at any given position within an approximate 500 m × 1 km vertical plane. The aircraft is considered to enter the wind field at a specified position under trimmed conditions. Both fixed control and automatic control landings are simulated. Flight paths, as well as control inputs necessary to maintain specified trajectories, are presented and discussed for aircraft having characteristics of a DC-8, B-747, and a DHC-6.

Nomenclature

C_L = lift coefficient, $L/(\frac{1}{2}\rho V_a^2 s)$
C_D = drag coefficient, $D/(\frac{1}{2}\rho V_a^2 s)$
C_m = moment coefficient, $M/(\frac{1}{2}\rho V_a^2 s\bar{c})$
$\bar{c}$ = chord length
D = drag
D_i = ($i = 1, 2, 3, 4, 5, 6, 7$) dimensionless constants
F_T = dimensionless thrust of the engines
FRL = fuselage reference line
g = magnitude of the acceleration of gravity
h_a = reference height 91.4 m
ILS = instrument landing system
I_{yy} = pitch moment of inertia
L = lift
L_T = effective moment arm of the thrust vector
m = aircraft mass
mg = gravitational force
M = pitching moment
$\dot{q}$ = time derivative of the pitching rate, q
s = wing area
V = dimensionless magnitude of the velocity relative to the Earth
V_a = dimensionless magnitude of the velocity relative to the air mass
$\mathbf{V}$ = dimensionless velocity vector relative to the Earth
$\mathbf{V}_a$ = dimensionless velocity vector relative to the air mass
W_x = wind speed horizontal to ground
W_z = wind speed vertical to ground
x = dimensionless distance parallel to the surface of the Earth
z = dimensionless distance perpendicular to the surface of the Earth (positive downward)
α = angle of attack
δ = angle between V_a and V
δ_E = elevator angle
δ_T = angle between the thrust vector and the fuselage reference line (FRL)
γ = flight path angle
γ' = angle of V_a relative to ground
$(\dot{})$ = derivative with respect to time
$(\,)_0$ = initial trimmed values

Received Nov. 27, 1978; revision received March 27, 1979.

Index categories: Aerodynamics; Guidance and Control; Atmospheric and Space Sciences.

*President; also Director, Atmospheric Science Div., University of Tennessee Space Institute, Tullahoma, Tenn. Member AIAA.

†Project Engineer, von Karman Gas Dynamics Facility. Member AIAA.

‡Research Engineer, Atmospheric Science Division, Space Sciences Laboratory.

Introduction

WIND shear associated with thunderstorm gust fronts is a serious hazard to aircraft operations in the terminal areas. Accidents in which wind shear has been identified as a contributing factor have occurred at Kennedy International Airport (Eastern Airlines),[1] at Stapleton Airport (Continental Airlines),[2] and at Logan International Airport (Iberian Airlines),[3] to mention only a few recent events. This paper investigates computer-simulated flight characteristics of two large jet commercial-type airliner and a STOL-type aircraft (i.e., having characteristics of a Twin Otter) landing through 11 separate wind fields associated with thunderstorm outflows. The influence of the wind field and the separate wind components individually on the aircraft flight path, pitch, airspeed, and other aerodynamic parameters is investigated. The analysis is carried out first, with the aircraft controls fixed in the trimmed conditions at entry into the flowfield, second, with an idealized automatic landing system, and finally, with a similar but simpler control system. The results of the study isolate and identify the influence of individual wind components and individual control inputs on landing through wind-shear characteristics of thunderstorm outflows.

Wind Shear

Eleven thunderstorm outflows measured from the 500 m meteorological tower at the National Severe Storms Laboratory in Norman, Oklahoma[4] have been converted to horizontal spatial coordinates with Taylor's hypothesis. The resulting two-dimensional wind field is tabulated on a 41×11 grid system and coupled with a computer lookup subroutine.[5]

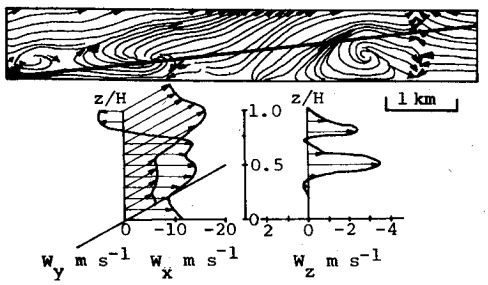

Fig. 1 Typical wind profiles along a −3 deg glide slope for thunderstorm case 9, $H = 7408 \tan 3$ deg, m.

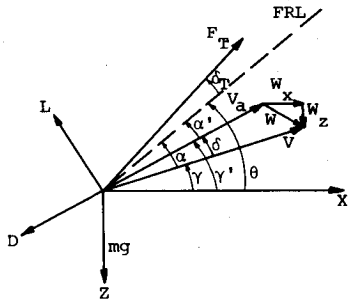

Fig. 2 Forces acting on a point mass aircraft and velocity relationships.

When the subroutine is called with the horizontal and vertical position of the aircraft (x,z), it returns the horizontal windspeed W_x, the vertical windspeed W_z, and the spatial wind gradients W_{xx}, W_{xz}, W_{zx}, and W_{zz} at that position. Figure 1 shows streamlines and the velocity components that would be encountered through a thunderstorm along the flight path indicated on the streamline pattern. The programmed wind fields combined with the three-degrees-of-freedom, longitudinal equations of motion governing aircraft flight allow the aircraft behavior to be evaluated in severe wind shear associated with thunderstorms.

Governing Equations of Motion

The aircraft is modeled as a point mass. A force balance perpendicular and parallel to the groundspeed velocity vector, Fig. 2, is employed to derive the following equations:

$$\dot{V} = -D_1 (C_D \cos\delta + C_L \sin\delta) V_a^2 - D_2 \sin\gamma + D_6 F_T \cos(\delta_T + \alpha) \tag{1}$$

$$\dot{\gamma} = [D_1 (C_L \cos\delta - C_D \sin\delta) V_a^2 - D_2 \cos\gamma + D_6 F_T \sin(\delta_T + \alpha)]/V \tag{2}$$

where the D_i's are defined as

$$D_1 = (\rho/2)(sh_a/m), \quad D_2 = gh_a^2/V_{a_0}^2, \quad D_3 = h_a^2/V_{a_0}^2$$

$$D_4 = \bar{c}/2h_a, \quad D_6 = gh_a F_{T_0}/mV_{a_0}^2$$

Other nomenclature is defined in Fig. 2. A moment balance gives:

$$\dot{q} = D_7 F_T + D_5 V_a^2 C_m \tag{3}$$

where

$$D_5 = (\rho/2)(s\bar{c}h_a^2/gI_{yy}) \qquad D_7 = L_T F_{T_0}/I_{yy}$$

with the remaining equations making up the complete set:

$$V_a = [(\dot{x} - W_x)^2 + (\dot{z} - W_z)^2]^{1/2} \tag{4}$$

$$V = W_x \cos\gamma - W_z \sin\gamma + [(W_z \sin\gamma - W_x \cos\gamma)^2 + V_a^2 - (W_a^2 + W_z^2)]^{1/2} \tag{5}$$

$$\sin\delta = (W_x \sin\gamma + W_z \cos\gamma)/V_a \tag{6}$$

$$\dot{\alpha}' = q - D_1 C_L V_a - [D_2 \cos\gamma' + D_6 F_T \sin(\delta_T + \alpha') + (\dot{W}_x \sin\gamma' + \dot{W}_z \cos\gamma')]/V_a \tag{7}$$

$$\dot{W}_x = \frac{\partial W_x}{\partial t} + V\left(\frac{\partial W_x}{\partial x}\cos\gamma - \frac{\partial W_x}{\partial z}\sin\gamma\right)$$

$$\dot{W}_z = \frac{\partial W_z}{\partial t} + V\left(\frac{\partial W_z}{\partial x}\cos\gamma - \frac{\partial W_z}{\partial z}\sin\gamma\right)$$

Inspection of the equations shows that wind shear enters explicitly only in Eq. (7). The term $\dot{W}_x \sin\gamma' + \dot{W}_z \cos\gamma'$ in this equation demonstrates that passing through a varying wind field results in a contribution to the rate of change in angle of attack. Of course variation in wind enters Eqs. (1) and (2) indirectly through V_a and δ [see Eqs. (4) and (6)]. The aerodynamic coefficients C_L, C_D, and C_m used in the analysis are those characteristics of a DC-8, B-747, and a DHC-6. An augmentor wing STOL aircraft is also considered in Ref. 6.

Automatic Control Systems

The control approach consists of a hold, capture, tracking, and flare mode. Two control systems are utilized in the study. Both systems employ variable gains for the servomechanism inputs:

$$F_{T_C} = K_{T1} V_a + K_{T2} \frac{\dot{z}}{V} + K_{T3} \frac{\dot{x}}{V} + K_{T4} \theta_c$$

$$\delta_{E_C} = K_{E1} V_a + K_{E2} \frac{\dot{z}}{V} + K_{E3} \frac{\dot{x}}{V} + K_{E4} \theta_c$$

where the gains K are determined during each time step of the landing by solving Eqs. (1-3) simultaneously for F_T, α', and δ_E.

The difference between the two control systems lies in the variables utilized in calculating the value of the gains. The control system referred to as the idealized automatic control loop assumes that the variables α', $\dot{\alpha}'$, δ, and q can be monitored during the approach and fed back into the control system to calculate the variable gains continuously along the glide slope. The idealized control loop also assumes that the groundspeed components $\dot{z}/V$ and $\dot{x}/V$ are available as feedback inputs to the servomechanisms for the thrust and elevator angle (see Fig. 3).

The "conventional" or simplified automatic control loop assumes that only the relative airspeed V_a is monitored during the approach and is available for computing the variable

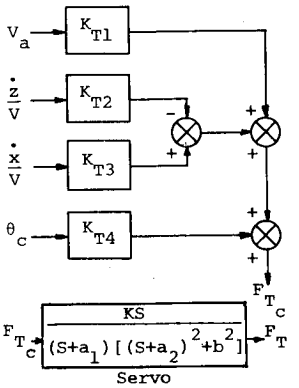

Fig. 3 Thrust servomechanism.

gains. Additionally, this control loop does not allow for $\dot{z}$ and $\dot{x}$ as feedback input, but rather expresses $\dot{z}/V$ as $-\sin\gamma$ and $\dot{x}/V$ as $\cos\gamma$. The value of γ was set equal to zero during the hold and flare modes and to the glide path angle during the capture and tracking modes.

Results and Discussion

The results of the study are first described for fixed controls and then for automatic controls. Initially, flight paths of all three aircraft were calculated for a fixed controls approach through the 11 different thunderstorms modeled. From this study, the two thunderstorms which were representative of extremes relative to flight paths which resulted in an overshoot or undershoot were selected and used for the follow-on comparison of the two automatic control systems and for analysis of the required control inputs, touchdown point, and other factors of interest in landing through thunderstorms.

Solution Technique

The governing equations are solved with a variable step size, multiple equation Runge-Kutta numerical integration scheme.[6] The initial conditions for all analyses are trimmed conditions at the point at which the aircraft enters the wind field. Typically, the point of entry is either at $z=91$ m or at $z=305$ m and toward the approaching storm gust front. For the majority of the storms considered, this results in the aircraft being normally trimmed for a light tailwind and updraft with subsequent flight into strong headwinds and fluctuating updrafts and downdrafts.

Fixed Controls

The flight paths of an aircraft characteristic of a DC-8 and a DHC-6 landing from a 305 m elevation with fixed controls along a -2.7 deg and -7 deg glide slope, respectively, are shown in Figs. 4 and 5. Those flight paths that are not carried out to completion are a result of the experimental data being insufficient to investigate landing to the touchdown point. Similar flight paths were obtained for aircraft having characteristics of a B-747 and an augmentor-wing STOL.[6] The STOL aircraft, however, was unable to negotiate many of the storm cases with fixed controls.

For the fixed stick approach, the aircraft was trimmed on the glide slope at the point of entry into the flowfield and the corresponding throttle and elevator angle settings were held constant for the remainder of the landing. The flight paths for thunderstorm models 9 and 11 are rather distinctive, as illustrated by Fig. 4, and these two thunderstorms were selected for the majority of the follow-on analyses.

Figure 6 is a comparison of fixed control cases 9 and 11 with the aircraft initially trimmed to follow a -2.7 deg glide slope. The aircraft involved are characteristic of DC-8, B-747, and DHC-6. For case 9, the phugoid oscillation of the aircraft is wildly excited. The frequency of oscillation for the aerodynamically similar DC-8 and B-747 is approximately the same, except for a slight phase shift. The oscillation of the slower, lighter DHC-6 is less pronounced, but still very much present. The nonlinear, computer-simulated values and the linear-predicted values of the phugoid period and characteristic wavelength are presented in Table 1. The predicted values for the phugoid period are given by Etkin[7] as $T=\sqrt{2}\pi V_a/g$. The phugoid wavelength λ is then found from $\lambda=VT$, and nondimensionalized as $\lambda=\lambda/h_a$, where $h_a=91$ m. Notice that values for a DC-8 and B-747 correspond closely with the linear-predicted values, but this relation does not hold true for the DHC-6. In the case 11 wind field, the aircraft do not display the pronounced phugoid oscillation experienced in case 9.

The windspeeds actually "seen" by the DC-8-type aircraft during landing for cases 9 and 11 wind fields are shown in Fig. 7. The windspeeds $\hat{W}_x$ and $\hat{W}_z$ are nondimensionalized with the initial airspeed V_{a_0}. A negative value for the longitudinal and vertical winds indicates a headwind or updraft; whereas a positive value represents a tailwind or downdraft, respectively. The wind profiles shown in the figure will be different, depending on the point within the flowfield that the flight of the aircraft begins. Beginning at different points in the wind field causes a change in the initial trim conditions of the

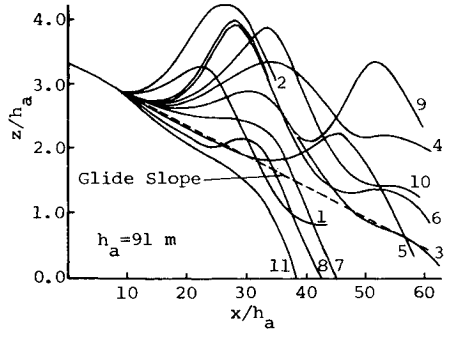

Fig. 4 Flight paths of DC-8-type aircraft landing with fixed controls from 305 m level, glide slope -2.7 deg.

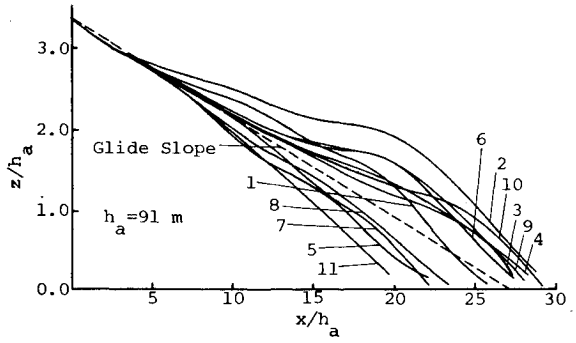

Fig. 5 Flight paths of DHC-6-type aircraft landing with fixed controls from 305 m level, glide slope -7.0 deg.

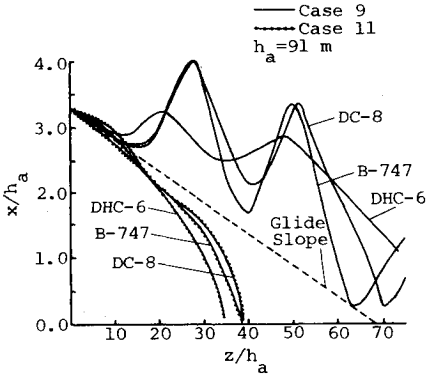

Fig. 6 Comparison of aircraft landing with fixed controls in thunderstorm cases 9 and 11 from 305 m level, glide slope -2.7 deg.

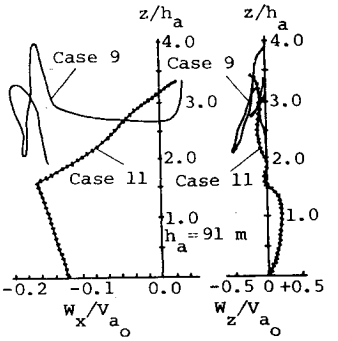

Fig. 7 Dimensionless winds "seen" by DC-8-type aircraft landing with fixed controls in thunderstorm cases 9 and 11.

Table 1 Phugoid period and horizontal wavelength

Aircraft type	V_a, m s^{-1}	T, s		λ, m		$\hat{\lambda}=\lambda/h_a$	
		Computed	Predicted	Computed	Predicted	Computed	Predicted
DC-8	70	29.9	31.7	2180	2203	23.84	24.09
B-747	66	28.8	30.0	2067	2085	22.60	22.80
DHC-6	46	27.1	20.7	2405	1016	26.30	11.11

aircraft. Inspection of Fig. 7 reveals that for case 11, headwinds increase at approximately the same rate as for case 9, but updrafts are not as severe. In case 11, a strong downdraft was encountered at the end of the horizontal shear; whereas for case 9, a strong updraft was encountered which forced the aircraft through a second oscillation. To separate the influence of updraft and downdrafts from the influence of variations in horizontal windspeed, the solution for case 9 was repeated first with $W_z=0$, and second with $W_x=0$. The resulting flight paths are shown in Fig. 8.

Figure 8 illustrates that the phugoid mode is excited by the horizontal wind shear from $15<x/h_a<40$, but is considerably less strongly influenced by the horizontal wind when the vertical component is absent as in the region of $x/h_a>40$. Recall, however, from Fig. 7 that the wind shear in the horizontal direction is essentially gone when the airplane is beyond $x/h_a>40$. The curve for the W_x case has only a very small excitation of the phugoid mode and, although causing an overriding of the glide slope and a long landing, does not cause the extreme oscillations with associated loss of airspeed and severe pitch angles found when both components are present. This observation tends to support the conclusion of McCarthy and Blick[8] and Blick et al.[9] that the characteristic windspeed wavelength of thunderstorms can cause instability in the phugoid mode.

They have shown that a horizontal gust produces a large peak in the aircraft velocity perturbation and a lesser peak in altitude perturbation at the aircraft phugoid frequency. This means that if a steady sinusoidal horizontal gust input on the order of 4 knots were encountered, the aircraft, depending on its aerodynamic characteristics, would respond with a sinusoidal velocity perturbation of approximately 40 knots. At one point in its cycle the aircraft would approach a stall speed or go below it during each sine wave cycle. They found that vertical sinusoidal gusts do not affect the aircraft velocity as much as horizontal gusts. They noted that 3 min. before Eastern flight 66 (Boeing 727) crashed at New York's Kennedy Airport on June 24, 1975, a light aircraft (Beechcraft Baron) made a successful landing, although it did experience a heavy sink rate and an airspeed drop of 20 knots. Their premise is that medium-sized jet transport aircraft tend to experience larger excursions in velocity and altitude when flying through horizontal gusts associated with thunderstorms because these gusts have large spectral components near the phugoid frequency. This is not the case for lighter aircraft.

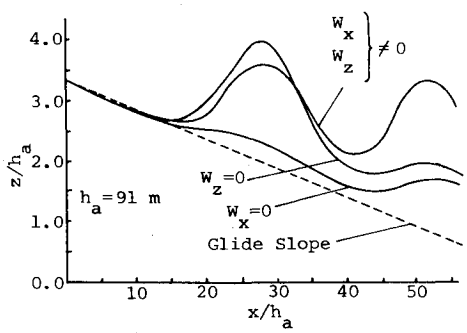

Fig. 8 Comparison of DC-8-type aircraft landing with fixed controls in thunderstorm case 9 considering individual wind components and both wind components.

This observation is in complete agreement with the results shown in Fig. 6.

On the other hand, Fujita[10] analyzed the same Eastern 66 accident and attributes the accident to a strong downburst encountered from flying through the center of the downdraft zone of the thunderstorm's cell. Figure 9 shows the flight path of a DC-8-type aircraft landing through the wind field associated with the Kennedy accident as tabulated for computer application by Keenan.[11] Results for the case of the total wind field (flight path A) and for the case where each wind component is individually set equal to zero are shown (flight path B, $W_x=0$; flight path C, $W_z=0$). On top of the figure are shown the windspeeds encountered along flight path A.

The interesting observation is that the downburst of approximately $W_z=12$ m s^{-1} at $x/h_a=18.5$ applied separately would cause the aircraft with fixed controls to crash at approximately $x/h_a=30$. However, when coupled with the increasing headwind, the aircraft manages to negotiate the severe downdrafts and land, although experiencing large amplitude oscillations. The horizontal wind shear component alone causes less severe flight conditions.

It appears that the combined effect of both wind shear components is important. Had the longitudinal windspeed been shearing out, i.e., a decreasing headwind, the aircraft would have landed even shorter. Therefore, the conclusions of Blick et al.[9] are not confirmed in this case. Further study is required to determine how longitudinal and lateral wind shears combine to create hazardous effects.

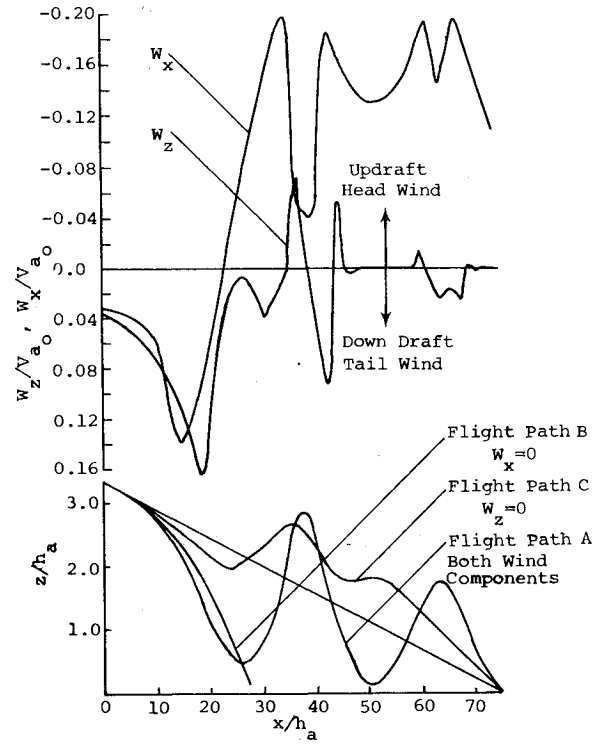

Fig. 9 DC-8-type aircraft landing with fixed controls in wind field associated with JFK Eastern 66 accident, and winds encountered along flight path A.

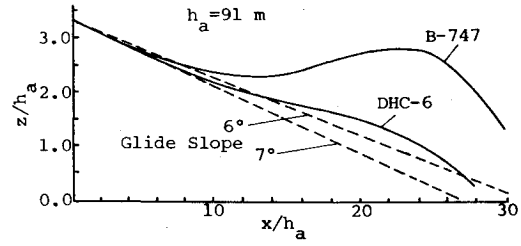

Fig. 10 Flight path comparison of aircraft landing with fixed controls from 305 m level with increased approach angle in thunderstorm case 9.

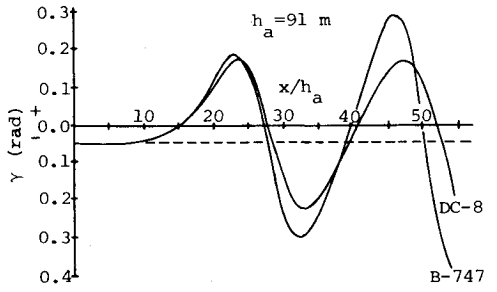

Fig. 11 Comparison of flight path angle of DC-8 and B-747 landing with fixed controls in thunderstorm case 9.

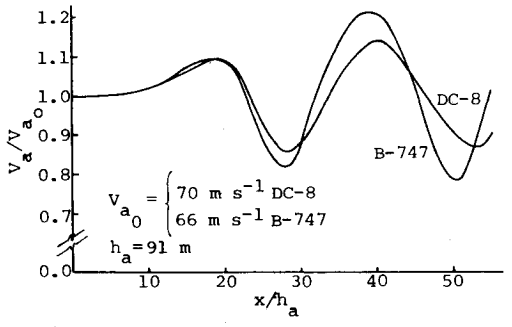

Fig. 12 Comparison of indicated airspeed of DC-8 and B-747 landing with fixed controls in thunderstorm case 9.

Inspection of Fig. 10 shows that the DHC-6 has a much more highly damped phugoid oscillation when landing at a −7 deg glide slope than is shown in Fig. 6 for landing at a −2.7 deg glide slope. This raises the question as to whether the influence of approach angle on the phugoid oscillation observed while landing through thunderstorms is a significant factor. (Note that the effect of γ is known to influence the phugoid oscillation.[7]) To ascertain this effect, the flight path of a B-747-type aircraft approaching at −6 deg is compared with that of a DHC-6-type aircraft approaching at −7 deg in Fig. 10. Damping of the phugoid oscillation of the B-747-type aircraft is achieved, but still relatively large oscillations about the expected flight path occur.

The flight path angle, γ, and indicated airspeed, V_a, for aircraft typical of the DC-8 and B-747 landing through two

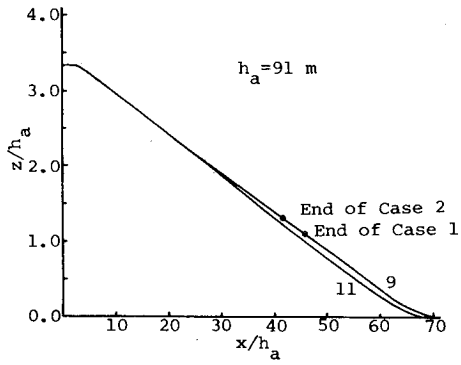

Fig. 13 Flight path comparison of DC-8-type aircraft landing with automatic controls in several different thunderstorm cases.

representative wind fields have been compared in Figs. 11 and 12, respectively.

Figure 12 shows the indicated airspeed nondimensionalized with the initial relative velocity V_{a_0} plotted against the nondimensionalized horizontal distance x. Figure 12 indicates that the airspeed reaches a low of 118 knots (61 m s^{-1}) twice for the DC-8 model, and two independent lows of 105 knots (54 m s^{-1}) and 100 knots (52 m s^{-1}) for the B-747. All four low points are attained at a pitch angle of 0 rad. The level stall speed for a DC-8 and a B-747 is 113 and 108 knots (57 and 55 m s^{-1}), respectively, which indicates the DC-8-type aircraft is operating at an unsafe margin above stall and the B-747 is below stall.

Tabulated values of the deviation from the expected touchdown point are presented in Table 2 to provide an indication of the severity of the wind shear effects in this regard. Many of the flights are forced to land short, a tragic event by any margin, as proved by examining wind shear related NTSB aircraft accident reports (see Refs. 1-3). Overshooting of the touchdown point is not as alarming since a go-around can almost always be executed.

The preceding results have shed light on the influence of thunderstorm wind shear on aircraft performance during approach. However, it is obvious that flight through severe wind shear would not be attempted with fixed controls, and the effect of automatic or feedback control systems on the airplane performance must be investigated. Results of applying the two different automatic control systems described earlier are given in the following section.

Automatic Control System

Approach simulations involving a DC-8 and a DHC-6 Twin Otter-type aircraft were conducted first with the "idealized" automatic landing system. Figure 13 shows the flight paths of the DC-8-type aircraft through thunderstorm cases 1, 2, 9, and 11. The control system aids the DC-8 in negotiating the severe wind shear extremely well, provided that unlimited control input is allowed. The thrust, F_T, required to maintain the glide path is shown in Fig. 14. The rate at which thrust must be changed exceeds engine capabilities on certain excursions and, therefore, a rate limiter was added to the automatic control program. An estimation spool time of 3600

Table 2 Deviation from expected touchdown point in meters

	Thunderstorm case number										
Aircraft	1	2	3	4	5	6	7	8	9	10	11
DC-8[a]	OD[d]	OD	−572	OS[c]	−983	OD	−2263	−2446	OS	OD	−2788
B-747[a]	OD	OD	−640	OS	−983	−686	−2355	−2583	OS	−550	−2880
Augmentor-wing STOL[b]	−946	OD	−901	OD	−727	OD	LP[e]	LP	OD	−690	−928
DHC-6 Twin Otter[b]	−82	+123	+55	+146	−288	+101	−479	−311	+101	+192	−597

[a] −2.7 deg glide slope. [b] −7.0 glide slope. [c] OS: severe overshoot—actual value not computed before exhausting data. [d] OD: out of data range. [e] LP: looped.

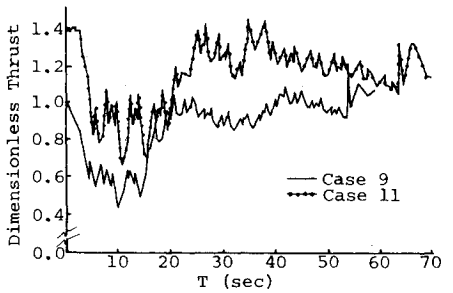

Fig. 14 Thrust requirements of a DC-8-type aircraft landing with an automatic control system in thunderstorm cases 9 and 11.

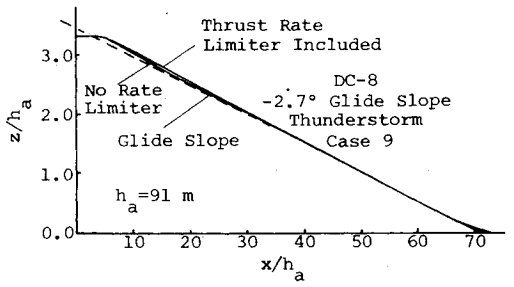

Fig. 15 Comparison of flight paths for DC-8-type aircraft with and without thrust rate limiter.

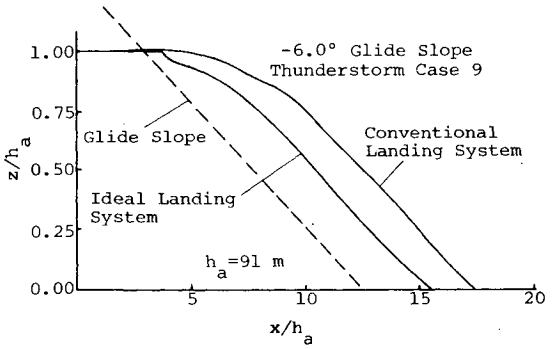

Fig. 16 Comparison of flight paths with idealized and more conventional control systems for DHC-6-type aircraft.

kg of thrust per second for the DC-8-type Pratt & Whitney JT3D turbofan engine was used. The approach paths followed with thrust rate limiters being utilized are compared with those having no thrust rate limitation in Fig. 15. The departure from the desired flight path trajectory of the DC-8-type aircraft without any limit on the maximum thrust is approximately 9 m; whereas with the limiter, the maximum departure is 20 m. The thrust rate-limited aircraft does not follow the ILS beam as closely in the earlier part of the landing, but both simulations do intercept the beam at approximately $x = 3200$ m, and track precisely along the beam flaring on target. The control inputs required for the elevator were investigated and appear to be readily achievable.

The "idealized" control system was compared with the more "conventional" landing system for the DHC-6-type aircraft. Figure 16 depicts the Twin Otter landing with the different control systems. The more conventional system does not provide as much control as the idealized landing system through the case 9 thunderstorm wind field. Neither simulation establishes the designated trajectory along the ILS beam glide path. This is due to the capture control parameters not being appropriately specified for the DHC-6-type aircraft. However, the tracking control does establish a well-defined trajectory which includes a successful landing, and the results shown in the figure are indicative of the control which can be achieved through rather severe thunderstorm wind shear with appropriate control systems.

Conclusions

The results of this study show that the phugoid oscillations of aircraft with fixed controls landing through typical thunderstorm gust fronts are highly amplifed. This is particularly true for the larger transport-type aircraft. The amplitude of the oscillations tend to be reduced for lighter-type aircraft typical of a DHC-6 Twin Otter. This is partly due to the characteristics of the aircraft and partly due to the steeper landing paths followed. The larger transport-type aircraft, approaching at steeper glide paths than those conventionally used in aviation operations, have somewhat damped phugoid oscillations, but still experience large excursions from the landing path. The strong influence of horizontal gradients in thunderstorm-associated wind fields on the phugoidal oscillation support the Blick et al.[9] hypothesis that accidents associated with commercial aircraft landing through thunderstorm gust fronts may result from the horizontal wind shear, but do not rule out that severe downburst can be equally responsible for accidents. Investigation of flight through the thunderstorm wind fields established by Fujita[10] indicate that the downburst can cause accidents. On the other hand, the downburst combined with the longitudinal wind shear for the one case studied, results in the aircraft negotiating the wind field. It does, however, experience severe oscillations.

Automatic control systems using variable gains can almost completely eliminate the severe perturbations from the flight path for the 11 thunderstorm models considered in this study. This does not imply that automatic control systems can be utilized to land aircraft through thunderstorms in all situations. The thunderstorm models utilized in this study are obviously not all inclusive and represent only the gust front portion. The automatic control systems have not been applied to the extreme downburst winds that have been reported to occur in the center of the thunderstorm cell.[10] Moreover, the computer simulation treats only three-degrees-of-freedom effects and, therefore, excludes additional control inputs required to stabilize roll and yaw motions.

The fact that the automatic control systems do, however, appreciably eliminate flight path excursions tend to support the arguments that accidents in thunderstorms are not a result of aircraft limitations, but often are precipitated during transition from automatic to manual control.[3]

Acknowledgments

The authors are grateful for the support of J. Enders, Chief of the Aviation Safety Technology Branch, Office of Aeronautics and Space Technology (OAST), and G. H. Fichtl, Chief of Fluid Dynamics Branch, Atmospheric Science Division, George C. Marshall Space Flight Center, Alabama.

References

[1] "Eastern Airlines, Inc., Boeing 727-225, John F. Kennedy International Airport, Jamaica, New York, June 24, 1975," National Transportation Safety Board, Washington, D.C., Aircraft Accident Rept. No. NTSB-AAR-76-8, March 12, 1976.

[2] "Continental Airlines, Inc., Boeing 727-224, N88777, Stapleton International Airport, Denver, Colorado, August 7, 1975," National Transportation Safety Board, Washington, D.C., Aircraft Accident Rept. No. NTSB-AAR-76-14, May 5, 1976.

[3] "Iberia Lineas Aereas de Espana (Iberian Airlines), McDonnell Douglas DC-10-30, EC CBN, Logan International Airport, Boston, Massachusetts, December 17, 1973," National Transportation Safety Board, Washington, D.C., Aircraft Accident Rept. No. NTSB-AAR-74-14, Nov. 8, 1974.

[4] Goff, R.C., "Thunderstorm Outflow Kinematics and Dynamics," National Severe Storms Laboratory, Norman, Okla., NOAA Tech. Memo. ERL NSSL-75, Dec. 1975.

[5]Frost, W., Camp, D.W., and Wang, S.T., "Wind Shear Modeling for Aircraft Hazard Definition," FWG Associates, Inc., report prepared uner Interagency Agreement No. DOT-FA76-WAI-620, supported by Federal Aviation Administration, Wind Shear Office, Dec. 1977.

[6]Frost, W. and Crosby, B., "Investigation of Simulated Aircraft Flight Through Thunderstorm Outflows," NASA Contractor Rept. 3052, Sept. 1978.

[7]Etkin, B., *Dynamics of Atmospheric Flight*, John Wiley and Sons, Inc., New York, 1972.

[8]McCarthy, J. and Blick, E.F., "Aircraft Response to Boundary Layer Turbulence and Wind Shear Associated with Cold-Air-Outflow from a Severe Thunderstorm," *Proceedings of the 7th Conference on Aerospace and Aeronautical Meteorology and Symposium on Remote Sensing from Satellites*, Nov. 16-19, 1976, pp. 62-69.

[9]Blick, E.F., McCarthy, J., Bensch, R.R., and Sarabudla, N.R., "Effect of Wind Turbulence and Shear on Landing Performance of Jet Transports," AIAA Paper 78-249, presented at the AIAA 16th Aerospace Sciences Meeting, Huntsville, Ala., Jan. 16-18, 1978.

[10]Fujita, T. and Caracena, F., "An Analysis of Three Weather Related Aircraft Accidents," research conducted at the Dept. of the Geophysical Sciences, University of Chicago, 1977.

[11]Keenan, M.G., personal communication, Oct. 1977.